Ghost resonance in the chaotic Chua's circuit

I. Gomes, M. V. D. Vermelho, and M. L. Lyra
Instituto de Física, Universidade Federal de Alagoas, Maceió AL 57072-970, Brazil
(Received 24 January 2012; revised manuscript received 11 April 2012; published 7 May 2012)

We experimentally investigate the ghost resonance phenomenon in the electronic circuit of Chua operating in the chaotic regime. The circuit can be stimulated to jump between two single-scroll attractors by an external periodic signal with an amplitude above an intrinsic threshold. For subthreshold signals, jumps between the chaotic attractors can be promoted by a superposed white noise. We show that the circuit output can exhibit a well-defined ghost resonance signature, i.e., a resonance on a frequency that is absent in a multicomponent input signal, when the amplitudes of the input components are properly related. Further, we show that ghost resonance can be induced by the Chua's circuit's own chaotic dynamics when it is driven by a suprathreshold multicomponent signal without the need of an external noise source.

DOI: 10.1103/PhysRevE.85.056201 PACS number(s): 05.45.Gg, 05.10.Gg, 05.40.Ca

I. INTRODUCTION

Noise-driven dynamical phenomena have attracted the attention of the scientific community over the last decades. In particular, stochastic resonance, which is the optimal detection of a subthreshold sinusoidal signal through an optimal noise level, has helped to change the traditional concept of noise as a disturber agent [1]. Recently, stochastic resonance has been used to explain a phenomenon that happens in the human ear known as the *missing fundamental illusion*. In this phenomenology, the human ear can perceive frequencies that are not present in the characteristic function of pressed notes [2–7]. This phenomenon has been studied in a neuron model [7] and compared with a general case of unharmonious tones used in the experiments of Schouten [8], where the complex tones were constructed adding pure tones uniformly displaced from an harmonic series. A resonance produced by noise in a simple neuron model was observed with good agreement with experiments. The missing frequency detected in the presence of noise has been termed the *ghost frequency* and it has been observed in different systems [9–12], a phenomenon nowadays referred as *ghost stochastic resonance*.

On the other hand, chaos concepts have turned out to be essential to understanding various nonlinear dynamical processes. They have been the subject of intense investigations in several systems, ranging from lasers [13] to the human heart [14]. The interaction between systems that exhibit chaos with external signals has been largely explored in the study of synchronization processes [15,16]. Particularly, the interaction between an external signal and a nonlinear system is important since the response can be especially dependent on the input signal form. Given a dynamical system, a frequent goal is to determine an external driving signal that forces the system to achieve some desired characteristic response [17].

In the present work, we explore the possibility of a chaotic system to exhibit ghost resonance. We will use the Chua's circuit as a prototype system exhibiting chaos to develop a detailed analog experiment aiming to characterize the main features related to the ghost resonance. We will show that the internal dynamics is responsible for displacements of the resonance frequencies with respect to the theoretically predicted values. Such displacement will be shown to reduce substantially when the external signal is properly tailored to match the threshold characteristics of the internal chaotic dynamics. We perform our investigation considering the influence of an external signal composed of a superposition of sinusoidal functions and white noise on the dynamics of the chaotic Chua's circuit on which stochastic resonance plays a fundamental role. After this preliminary analysis, we will show that ghost resonance can be driven by the nonlinear dynamical system's own chaotic behavior, even in the absence of an external noise source.

The manuscript is organized as follows: In the next section, we will review some basic aspects of the stochastic and ghost resonances. In Sec. III, we describe the main characteristics of the Chua's circuit that are relevant to the present study. In Sec. IV, we present our analog experimental study for the Chua's circuit system driven by an external multicomponent subthreshold signal in the presence of external noise. Section V shows that the identification of ghost resonance can be done even in the absence of noise when the system is stimulated by a complex suprathreshold signal. In Sec. VI, we summarize and draw our conclusions.

II. STOCHASTIC AND GHOST RESONANCES

Stochastic resonance refers to a nonlinear phenomenon in which a dynamical system, benefited by an external noise, can respond to a subthreshold signal [1]. Usually, these systems depict a threshold which makes them unable to capture the presence of an external periodic harmonic stimulus with an amplitude weaker than the specified threshold. When noise is superposed to a subthreshold signal, stochastic crossings of the minimum stimulus level take place. However, for very weak noise amplitudes, these crossings only occur in the rare events of strong noise signals, with no correlation with the underlying periodic stimulus. Therefore, the system response does not bring any information from the typical frequency of the subthreshold signal. On the other hand, in the regime of strong noise amplitudes, the threshold crossings are promoted by the frequent events of large noise input. Once again, the system's response is insensitive to the underlying harmonic stimulus. At intermediate noise amplitudes, the level crossings occur more frequently when large noise and maximum of the periodic stimulus combine. In this way, although the sequence of crossings remains stochastic, it

depicts a pronounced frequency component matching that of the underlying harmonic stimulus.

There is a typical noise amplitude at which the recognition of the subthreshold signal is optimal, which is termed the stochastic resonance condition. It can be obtained by traditional time-series analysis techniques. A commonly used method is to compute the power spectrum of the system response and to measure the signal-to-noise ratio at the frequency corresponding to the subthreshold signal as a function of the noise amplitude. Such signal-to-noise ratio has a well-defined maximum at the optimal stochastic resonance condition. An alternative approach is to construct histograms of the frequencies at which the crossings occur. Near the stochastic resonance condition, it displays a well-defined maximum that identifies the frequency of the periodic stimulus.

Ghost resonance is a variant of the stochastic resonance phenomenon in which the periodic stimulus is a superposition of higher harmonics, equally spaced in frequency, of a fundamental tone [3]. When the maximum of this complex signal is below a response threshold, a stochastic resonance condition can be reached in the presence of noise. However, the main stochastic resonance is not in any of the frequencies contained in the periodic stimulus but rather in the missing fundamental tone. This phenomenon is referred to as the missing fundamental illusion, or ghost stochastic resonance, because the perceived tone corresponds to the fundamental frequency for which there is no actual source. This phenomenon has been shown to be directly related to pitch perception of complex sound waves [4–6]. Within this context, a relevant question refers to the shift in the pitch perception when the frequencies of the harmonic tones are rigidly displaced, which makes them no longer higher harmonics of a fundamental tone. Within this context, the external complex stimulus is usually considered as a superposition of sinusoidal functions in the form

$$F(t) = P[\sin(2\pi f_1 t) + \sin(2\pi f_2 t) + \ldots + \sin(2\pi f_n t)], \tag{1}$$

where $f_1 = kf_0 + \Delta f$, $f_2 = (k+1)f_0 + \Delta f, \ldots$, $f_n = (k+n-1)f_0 + \Delta f$; Δf is a frequency shift from a perfect harmonic series, f_0 is the fundamental tone, and P is the amplitude of the signal components. A stochastic resonance is observed in frequencies given by Ref. [3]

$$f_r = f_0 + \Delta f/[k + (n-1)/2], \tag{2}$$

where $n = 1,2,3\ldots$ and $k > 1$. The above equation actually corresponds to the expected frequency at which the highest peaks of the complex signal occur. Such prediction has been probed in several physical systems such as the FitzHugh-Nagumo neuron (FHN) model [7], lasers [9], and electronic systems [10]. It has also been well reproduced in experiments of pitch perception [8]. A recent review on ghost stochastic resonance and its different manifestations can be found in Ref. [3].

III. THE CHUA'S ELECTRONIC CIRCUIT

Here, we used an electronic circuit of Chua [18,19] due to its well-known characteristics, simplicity of construction, and capacity to exhibit a variety of bifurcations and chaos. Stochastic resonance has been numerically and experimentally observed in this system [20–23]. Our aim is to explore the behavior of this simple nonlinear dynamical system to study the main characteristics of the ghost resonance phenomenon in the presence of chaos.

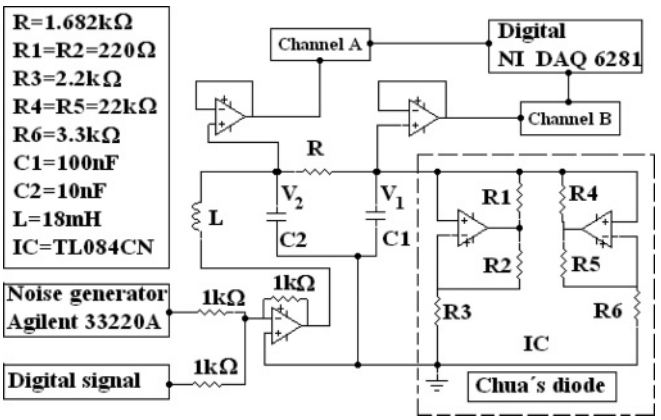

FIG. 1. Experimental setup. A Chua's chaotic circuit driven by superposed periodic signal and white noise.

The circuit diagram of the Chua circuit, as shown in Fig. 1, can be briefly described as consisting of five circuit elements. The first four elements are standard linear passive electrical components (L, R, C1, and C2) and the other is a nonlinear active element. The temporal dynamical behavior of the interconnected passive elements always leads to trivial solution of voltages and currents tending to zero. Chaotic or oscillatory trends occur with the inclusion of the fifth locally active element whose current shows a nonlinear dependence on its applied voltage, such as the Chua diode. The nonlinear function slope must be negative somewhere on the curve. The Chua's diode consists of two operational amplifiers, usually encapsulated in the same integrated circuit (IC) to avoid different thermal fluctuations, connected in the current feedback configuration. In the present investigation the input signals are a sum of a broadband white noise and a superposition of sinusoidal functions. The white noise is due to a function generator (Agilent 33220) and the superposition is digitally generated. This signal is applied to the circuit via the inductor L. The chaotic signals were measured by means of the voltages of the capacitors C1 and C2, respectively. The data acquisition system employed in the characterization consists of a 16-bit analog-to-digital card (ADC)—NI PCI6281 (500 kS/s)—connected to a personal computer (PC). Appropriated software was also used for data processing. A sampling frequency of 20 kHz was used during the experiments.

In the absence of sinusoidal and noise signals, the autonomous Chua's circuit exhibits chaotic dynamical behavior for the parameters of the electronic components we used. The phase space is characterized by two symmetric attractors called single scrolls [see Fig. 2(a)]. The dynamical trajectory selects one of two single scrolls depending on the initial condition of the circuit. The characteristic frequency of rotation of the dynamical trajectory around the single scroll is 2.8 kHz. The corresponding output signal is shown in Fig. 2(b). In the presence of an external perturbation, the system can be able to bifurcate and the phase space will exhibit the double-scroll chaotic attractor shown in Fig. 2(c). Under this

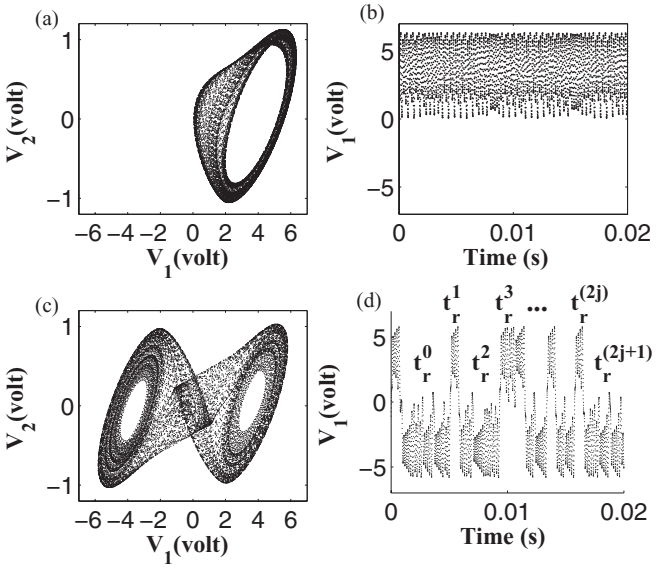

FIG. 2. (a) Single-scroll chaotic attractor. (b) Voltage V_1 as a function of time in the absence of external perturbation. (c) The system is driven by an external sinusoidal signal of frequency $f =$ 30 Hz reaching the double-scroll chaotic attractor. (d) Voltage V_1 as a function of time when the circuit is driven by a suprathreshold sinusoidal signal. The system jumps between the single scrolls. The series of $t_{r,j}$'s represent the stochastic sequence of residence times.

condition, the system exhibits a sequence of irregular jumps between the single scrolls [as shown in Fig. 2(d)].

As a preliminary step toward the study of ghost resonance in the Chua's circuit, we analyze under which conditions it can show stochastic resonance; i.e., we determine the optimal noise amplitude at which the system becomes able to detect subthreshold periodic sinusoidal signals [1]. The verification of stochastic resonance in a Chua's circuit operating in the chaotic regime has been well characterized in Ref. [23]. In general, there are some basic ingredients involved in the stochastic resonance of a nonlinear dynamical system. There is an amplitude threshold level below which the system is unable to detect a periodic external signal. In the Chua's circuit the threshold separates single- and double-scroll chaotic orbits. When the external sinusoidal signal $A\sin(2\pi ft)$ has a small amplitude, the system remains trapped in a single-scroll attractor. Jumps between the symmetric single scrolls are performed when the amplitude of the sinusoidal signal surpasses a threshold level A_s.

In the Chua's circuit, the threshold amplitude decreases continuously with the frequency of the harmonic signal in the frequency range we analyzed, as shown by the squared symbols in Fig. 3. Stochastic jumps can be produced when noise is superposed on a subthreshold sinusoidal signal. However, if the noise amplitude is too small or two large, these jumps occur at times that are uncorrelated to the modulations of the underlying periodic signal and no signature of its presence can be inferred from the system's dynamics. However, at intermediate noise levels, jumps are more probable to occur when the subthreshold signal is maximum. In this regime, the sequence of jumps is strongly correlated to the modulation of the underlying external signal and a time-series analysis

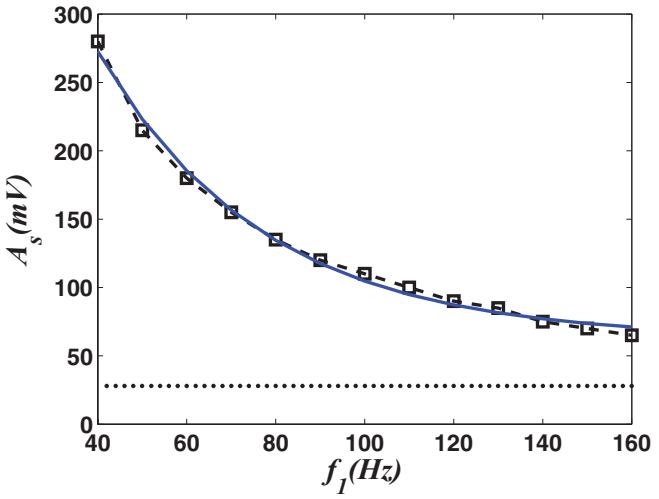

FIG. 3. (Color online) Squares: Frequency dependence of the threshold amplitude of an harmonic input signal $A\sin(2\pi f_1 t)$ versus frequency f_1. Solid line is an exponential fit of data in the form $A_s = a + be^{-\alpha f_1}$. Dotted line: The constant amplitude $P = 28$ mV used in the experimental results reported in Fig. 4(a).

of the system output can reveal its presence. Actually, there is an optimal noise amplitude at which the signature of the underlying subthreshold signal is more pronounced. Such optimal noise amplitude can be extracted by computing the maximal signal-to-noise ratio of the output spectral density or from frequency histograms derived from the residence time series.

IV. GHOST STOCHASTIC RESONANCE IN THE CHUA'S CIRCUIT

A. Interaction with an external periodic signal with $n = 2$ components

As emphasized in the previous section, stochastic resonance usually appears in systems with an activation threshold. The ideal setup is to stimulate the system with a subthreshold periodic signal which, by itself, is not able to make the system surpass the activation barrier. In the presence of noise, random jumps over the threshold are promoted which may bring information concerning the typical frequency of the underlying periodic signal. However, if the external periodic signal is too weak, the sequence of jumps becomes uncorrelated and the resonance signal is absent. Therefore, the external signal shall have an amplitude smaller than the threshold, but close enough to it to be detected by stochastic resonance.

In the case of Chua's chaotic system, the threshold depends on the frequency of the external sinusoidal signal, as seen in Fig. 3. Above the dashed line connecting the squares, the system jumps from one single scroll to another just due to the periodic sinusoidal signal $A\sin(2\pi ft)$. Below this line, the system remains trapped in a single scroll.

The frequency dependence of the threshold strongly affects the ghost resonance verification in the Chua's chaotic system. For example, consider Figs. 4(a) and 4(c) where we present the histograms of the experimental response of the system driven by a signal composed of two superposed sinusoidal

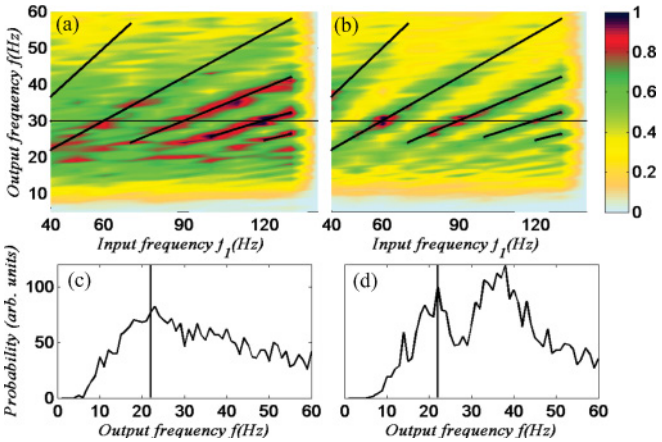

FIG. 4. (Color online) (a) Density plot of the frequency histograms when the system is driven by an external periodic two-component signal $P[\sin(2\pi f_1 t) + \sin(2\pi f_2 t)]$ of constant amplitude ($P = 28$ mV) superposed on a white optimal noise $N = 0.9$ V. Here $f_2 = f_1 + f_0 = 3f_0 + \Delta f$, with $f_0 = 30$ Hz and Δf ranging from -20 Hz to 70 Hz. Solid lines are the theoretically predicted ghost resonances. (b) Density plot of the frequency histograms when the system is driven by a two-component periodic signal with distinct amplitudes $P[\sin(2pif_1 t) + (A_s^2/A_s^1)\sin(2pif_2 t)]$ and white noise. Here P depends on the value of frequency shift Δf and is set below the frequency-dependent threshold level P_s (shown in Fig. 5). The values of A_s^2/A_s^1 are the ratio of the threshold amplitudes of each component. (c) and (d) show the histograms of the output frequencies for the cases of components with the same (c) and different (d) amplitudes. These have been obtained for the particular case of $f_1 = 40$ Hz. In (c) and (d) the vertical lines represent the theoretically predicted ghost frequency.

components with the same amplitude $P[\sin(2\pi f_1 t) + \sin(2\pi f_2 t)]$ and optimal noise amplitude $N = 0.9$ V. In Fig. 4(a), we have chosen f_1 to be on the horizontal axis and the output frequency f to be on the vertical axis. In this figure, the density plot is obtained by computing the histograms of the typical frequencies f_j of jumps between the single scrolls in the output signal V_1 (Figs. 1 and 2). f_j was obtained by taking the inverse of the sum of consecutive residence times $t_r^j + t_r^{j+1}$. The histograms were obtained by counting the number of occurrences of f_j within a window of 1 Hz. The vertical line in Figs. 4(c) and 4(d) marks the point where the main ghost frequency should arise according to theoretical arguments [3]. The parameters used to build the external two-component signal were $P = 28$ mV (below the threshold of the highest frequency component), $f_0 = 30$ Hz, $k = 2$, and $n = 2$; Δf varied from -20 Hz to 70 Hz. The peak in the histogram is the signature of the ghost resonance phenomenon.

In Fig. 4(a), although the general structure is in agreement with the theoretical prediction for the location of the ghost frequencies, we verify that there are small differences between the predicted and experimental values. Further, the histograms do not have a well-defined peak structure, thus exhibiting a weak sensibility to the stochastic resonance condition. These two aspects are directly related to the frequency dependence of the threshold. When the system is driven by a signal with two components with the same amplitude, the experiment shows that the circuit responds predominantly to the signal component which requires the smaller amplitude to promote the jumps between the single-scroll attractors. Therefore, the second component f_2 is always closer to its threshold, thus leading to the frequency displacements from the ghost resonance prediction. The first component f_1 does not have sufficient amplitude to significantly influence the dynamic response of the system because it is too far from the threshold and, therefore, from the internal resonance zone. These features make the system weakly sensitive to the ghost stochastic condition.

Based on the above discussion, we propose that a better ghost resonance signal can be obtained by taking advantage of the internal dynamics of the system when constructing the complex external signal. The main idea is to allow both components to have amplitudes close to their respective thresholds. In what follows, we will consider the external two-component periodic signal to be in the form

$$F(t) = P\sin(2\pi f_1 t) + Q\sin(2\pi f_2 t), \tag{3}$$

where P and Q allow us to adjust the individual intensity of the components and $s = 1,2,\ldots,n$ denotes their dependence on the frequencies $f_1 = kf_0 + \Delta f$ and $f_2 = (k+1)f_0 + \Delta f$ for different values of the frequency shift Δf. In order to choose the best ratio between the amplitudes of the two components, we observe that each of them has a distinct threshold level when acting individually, namely A_s^1 and A_s^2 for the frequencies f_1 and f_2, respectively. Using the parameters $f_0 = 30$ Hz, $k = 2$, with Δf ranging from -20 Hz to 70 Hz, we determined the values of A_s^1 and A_s^2. In the case of both components acting together, the best condition to achieve the ghost resonance is when their amplitudes are equally close to their respective thresholds. In this way, we consider these amplitudes to have the same ratio as the threshold levels by considering $Q = (A_s^2/A_s^1)P$.

Even with both components having amplitudes proportional to their respective thresholds, the complex signal still depicts a frequency dependence of its threshold amplitude P_s. In Fig. 5, we report the values of the threshold amplitude ratio A_s^2/A_s^1, as well as the overall threshold amplitude P_s as a function of the frequency shift Δf. Besides reporting the threshold for the case of two superposed components, we also report the threshold for a more complex signal containing $n = 4$ components that will be explored in the next subsection. The ghost stochastic resonance signal can then be optimized for each frequency displacement by choosing the overall amplitude of the complex signal to be nearly below its respective threshold.

The above procedure was implemented to analyze the ghost resonance phenomenon in the Chua's circuit, as shown in Figs. 4(b) and 4(d). Notice that the typical histogram now has a narrower well-defined peak at the theoretically predicted ghost frequencies, as seen in Fig. 4(d). The density plot [Fig. 4(b)] better characterizes the improvement of this approach as compared to the one using a periodic signal with two superposed components with identical amplitudes. We can see that the displacements from the predicted resonances have considerably decreased, with the peaks of the histograms well centered at the theoretical values.

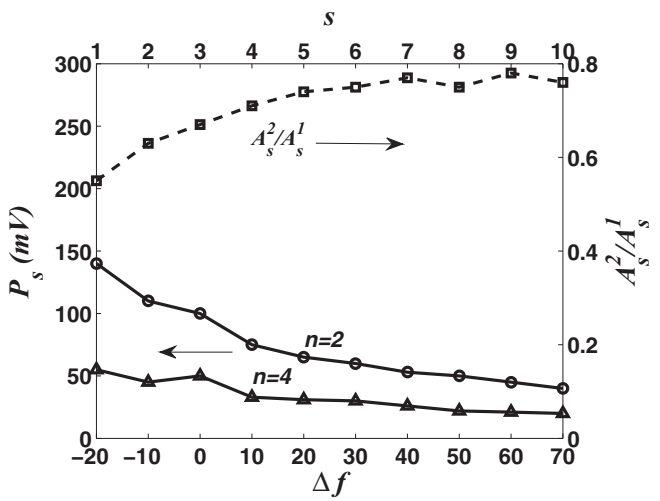

FIG. 5. Ratio between the threshold amplitudes A_s^2/A_s^1 of individual components, as well as the thresholds P_s of the $n = 2$ and $n = 4$ components signals having distinct amplitudes, versus the frequency shift Δf. Here $f_1 = 2f_0 + \Delta f$ and $f_2 = 3f_0 + \Delta f$ with $f_0 = 30$ Hz. 10 distinct frequency shifts are shown, indicated by the index s. The thresholds for the $n = 2$ components signal were used to obtain the experimental results reported in Fig. 4(b), while the thresholds for the $n = 4$ components signal were used to obtain the results reported in Fig. 6.

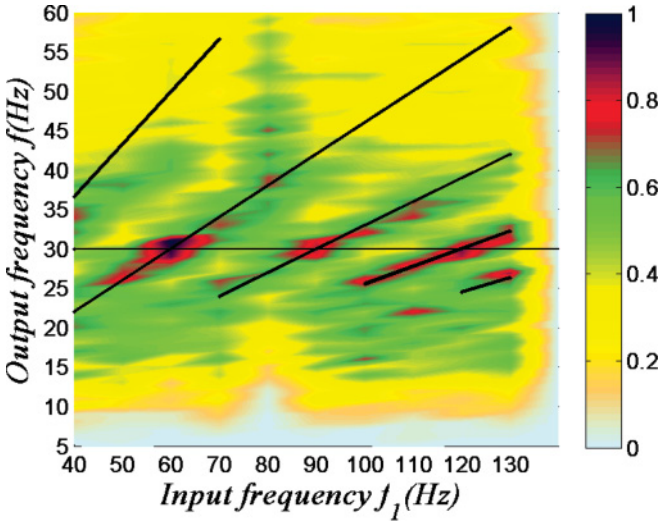

FIG. 6. (Color online) Density plot of the frequency histograms of the output signal for the case of a complex sub-threshold input periodic signal with $n = 4$ components. The peaks of the histograms still depict good agreement with the theoretical prediction for the location of the ghost frequencies (solid lines). Here $f_n = f_1 + (n - 1)f_0$, with $f_0 = 30$ Hz and we used the same noise level as in Fig. 4.

We would like to stress that although we have used distinct amplitude ratios for each frequency shift, they vary over a very limited range. We have experimentally checked that a ghost resonance signal with a similar accuracy can be achieved if, instead using the actual threshold amplitude ratio for each frequency shift, one simply uses the average threshold ratio over the entire experiment, as will be employed in the following.

B. Interaction with a complex signal with $n = 4$ components

The same methodology developed in the last section can be applied when the system is driven by a complex signal containing more than two components. In order to obtain a well-defined signature of the ghost resonance, we generalize the form of the input signal to account for the decay of the threshold amplitude at each frequency present in the complex signal. Within this line, the input signal is considered to be given by

$$F(t) = P[\sin(2\pi f_1 t) + \left(A_s^2/A_s^1\right)\sin(2\pi f_2 t) + \ldots + \left(A_s^n/A_s^1\right)\sin(2\pi f_n t)]. \quad (4)$$

We have driven the chaotic Chua's circuit using the above input signal superposed to a white noise to verify the ghost resonance phenomenon for the particular case of a signal containing $n = 4$ components. We have used the same parameters as in Fig. 4(b). However, in this case, we took the ratio between the threshold amplitudes as the average over all frequency shifts analyzed. Therefore the relative amplitude ratio of the signal components was taken as

$$F(t) = P[\sin(2\pi f_1 t) + 0.72\sin(2\pi f_2 t) + 0.56\sin(2\pi f_2 t) + 0.48\sin(2\pi f_2 t)]. \quad (5)$$

In this way, only the overall input amplitude P was adapted for each frequency shift in order to leave the input signal nearly below the activation threshold P_s of jumps between the single-scroll attractors, shown as triangles in Fig. 5. The density plot of the frequency histograms contained in the output signal is shown in Fig. 6. Note that the general structure is similar to the one reported in Fig. 4(b) for the case of a two-component input. There is a very good coincidence of the histogram peaks with the theoretically predicted values of the ghost frequency (shown as solid lines). This result is in agreement with previous observations of ghost resonance signals in several nonlinear stochastic systems on which the structure of the frequency histograms of the system's response is independent of the number of sinusoidal components present in the external signal.

Finally, we have observed that within the range of frequencies used in our experiments, the threshold amplitude of each sinusoidal component is well fitted by an exponential decay as a function of the signal frequency (shown as a solid line in Fig. 3). Therefore, a simple way to construct a complex external signal that can produce a well-defined signature of the ghost resonance phenomenon is to assume that $A_s^n/A_s^1 = \gamma^{n-1}$ for all frequency shifts. We will use this approach in the next section when discussing the possibility of identifying the ghost resonance signature in the Chua's circuit even in the absence of external noise.

V. GHOST RESONANCE WITHOUT NOISE

When the amplitude of the input periodic signal is above the activation threshold, jumps between the single-scroll attractors can occur without the assistance of an external noise. A relevant question to answer is whether a nonlinear chaotic system can depict the missing fundamental illusion under

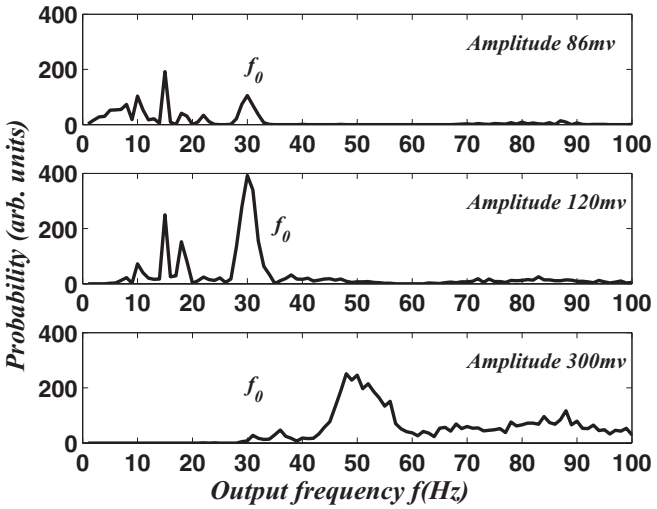

FIG. 7. Histogram of the frequencies contained in the output signal V_1 when the system is stimulated by a two-component signal with an overall amplitude above the activation threshold. The signal frequencies are $f_1 = 60$ Hz and $f_2 = 90$ Hz. The histogram shows a resonance in the missing fundamental frequency $f_0 = 30$ Hz for amplitudes not far above the threshold.

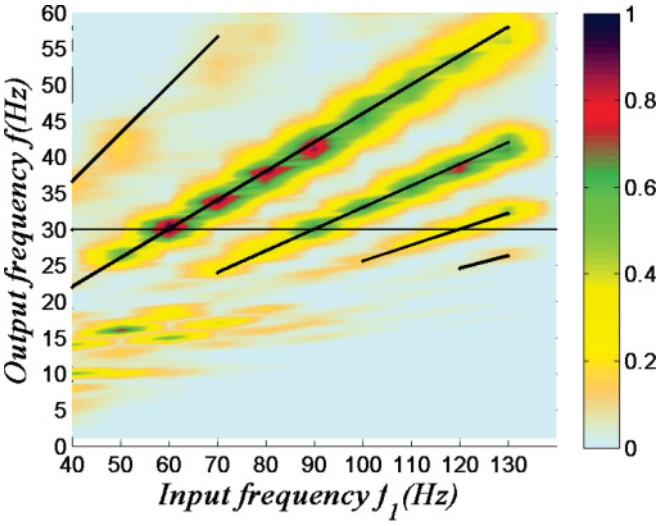

FIG. 8. (Color online) Density plot of the frequency histogram of the output signal when the Chua's circuit is driven by a suprathreshold two-component external signal without noise. Here we used both components with amplitude $P = 120$ mV, and $f_2 = f_1 + f_0$ with $f_0 = 30$ Hz. The solid lines show the theoretical prediction of the ghost frequencies.

this circumstance. In order to explore this point, we have firstly stimulated the chaotic Chua's circuit with a periodic signal presenting two components with identical amplitudes $F(t) = P[\sin(2\pi f_1 t) + \sin(2\pi f_2 t)]$ with $f_1 = 60$ Hz and $f_2 = 90$ Hz. The overall amplitude was varied above the threshold level. In Fig. 7 we plot the histogram of the output signal frequencies for three representative values of the input amplitude. One can clearly notice that a resonance at $f_0 = 30$ Hz appears for amplitudes nearly above the threshold. This is exactly the missing fundamental illusion, namely, a resonance at a fundamental frequency that is not present in the complex input signal. Its signature is more evident at intermediate amplitudes. In the present case, the signal amplitude resulting in the highest peak on the histogram at the missing fundamental frequency is around $P = 120$ mV.

In order to verify whether the missing fundamental frequency appearing in the case of suprathreshold signals depicts the expected dependence on a uniform shift of the signal frequencies, we drove the system by a two-component suprathreshold signal with frequencies uniformly shifted such that $f_2 = f_0 + f_1 = 3f_0 + \Delta f$. In Fig. 8 we show the density plot of the frequency histograms of the output signal. The peaks in the histograms present very good agreement with the theoretical prediction for the resonance frequencies (solid lines). Therefore, in this case of a suprathreshold two-component signal, there is no need to scale the signal components to properly detect the ghost resonance signature.

We extended the above analysis for a $n = 4$ components signal. When keeping all components with the same amplitude, the optimal overall amplitude to observe the ghost resonance signature is reduced to $P = 55$ mV. This is related to the fact that the highest frequency component has a smaller threshold (as shown in Fig. 3). The resulting density plot of the frequency histograms is reported in Fig. 9. For an input signal with $n = 4$ components, these peaks were expected to fall along straight lines with slopes given by the inverse of semi-integers [see Eq. (2)]. However, the data show that the peaks follow straight lines with slopes given by the inverse of integer numbers, as should be the case of an input signal with an odd number of components. This feature has the same origin of the resonance displacement reported in the case of subthreshold signals. The amplitude thresholds of the components with the lowest

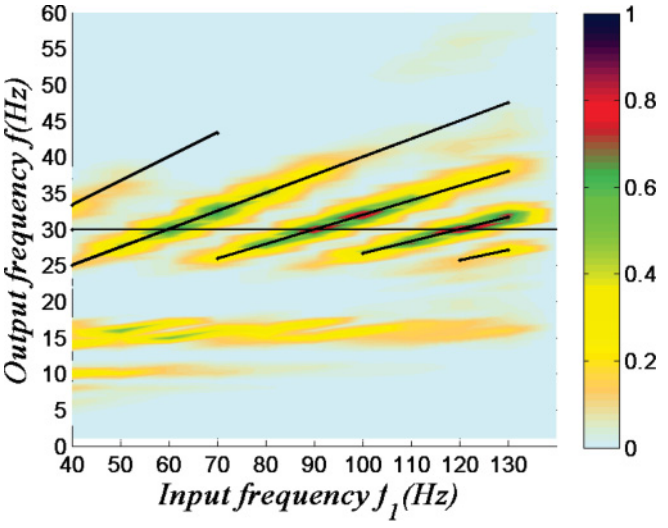

FIG. 9. (Color online) Density plot of the output signal frequency histograms when the Chua's circuit is stimulated by a suprathreshold signal with $n = 4$ components with the same amplitude $P = 55$ mV. Here we used $f_n = f_1 + (n-1)f_0$, with $f_0 = 30$ Hz. The straight lines have slopes given by the inverse of integer numbers, as would be expected for a complex input signal with an odd number of components. This feature indicates that the input components are not contributing on the same level to the dynamical mechanism of ghost resonance.

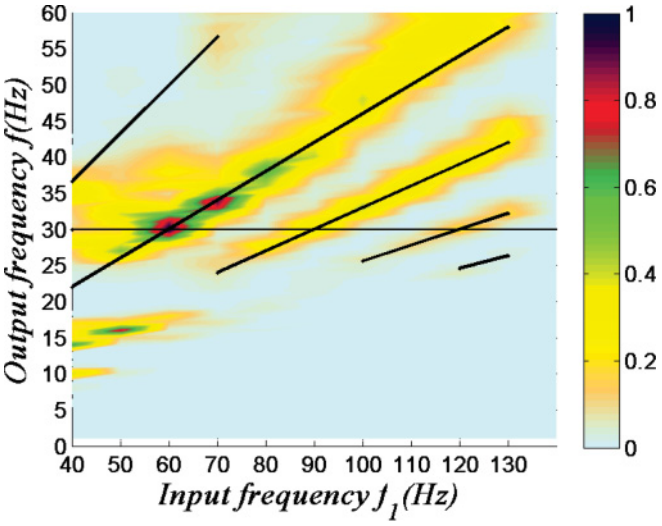

FIG. 10. (Color online) Density plot of the output signal frequency histograms when the Chua's circuit is stimulated by a suprathreshold signal with $n = 4$ components with amplitudes obeying $A_n/A_{n-1} = \gamma = 0.5$. The amplitude of the lowest frequency component was $P = 210$ mV. Frequencies are the same as in Fig. 9. In this case, there is a very good agreement between the experimental and theoretical location of the ghost resonance frequencies. The straight lines have slopes given by the inverse of semi-integers, as expected for a complex input signal with an even number of components.

and highest frequencies are quite distinct and they are not contributing on the same level to the dynamical mechanism of ghost resonance.

In order to overcome this point, we drive the system with a complex signal on which the components have relative amplitudes following the frequency dependence of the threshold. Based on the roughly exponential decay observed for the threshold in the small frequency regime we are probing (as shown in Fig. 3), we drove the system with an input signal of the form

$$F(t) = P[\sin(2\pi f_1 t) + \gamma \sin(2\pi f_2 t) + \gamma^2 \sin(2\pi f_3 t) + \gamma^3 \sin(2\pi f_4 t)]. \quad (6)$$

In Fig. 10 we report the density plot of the output frequency histograms for distinct frequency shifts of a $n = 4$ components input signal with $\gamma = 0.5$. Here, we also considered $k = 2$ in such a way that the lowest frequency present in the input signal corresponds to a shift of the second harmonic of the fundamental frequency $f_0 = 30$ Hz. The frequency shift was also varied from -20 Hz up to 70 Hz. We have observed in this study that the overall amplitude of the input signal, at which the ghost resonance signature is optimal, is $P = 210$ mV. With this properly tailored input signal, on which all components play a similar role in the system's dynamics, we got a very good agreement between the experimental and theoretical values, with the ghost resonance frequencies falling along straight lines with slopes given by the inverse of semi-integers.

VI. SUMMARY AND CONCLUSIONS

In summary, we performed an experimental analog study of the ghost stochastic resonance in the chaotic Chua's circuit driven by a multicomponent external signal. For external signals with an amplitude below a threshold level, the dynamical attractor is a single scroll. When the system is stimulated by a subthreshold signal, jumps between two symmetric single scrolls can be activated by a superposed white noise. In the chaotic Chua's circuit, the threshold level of a sinusoidal signal depends on its frequency. Therefore the distinct components of a complex signal can play different roles in the dynamics. We have shown that when the Chua's circuit is driven by a superposition of a subthreshold multicomponent signal and white noise, the output signal can display the ghost resonance phenomenon, on which the system responds in a frequency that is not present in the input signal, related to a missing fundamental component. Due to the frequency dependence of the threshold level, we have found that the ghost resonance signature is deteriorated when the system is driven by a complex signal on which all components have the same amplitude. In this case, the output frequency histograms do not depict well-defined peaks and the location of the experimental peaks are displaced with respect to the theoretically predicted ghost frequencies. We have shown that a very well defined ghost resonance signature can be achieved when the amplitudes of the input signal components decay with frequency following the corresponding decay of their individual threshold levels. Finally, we experimentally observed that ghost resonance can still be identified without the need of an external noise for suprathreshold signals. These results corroborate the recently developed concept that ghost resonance is a ubiquitous phenomena presented by nonlinear dynamical systems.

ACKNOWLEDGMENTS

We would like to thank CAPES, CNPq, and FINEP (Brazilian research agencies) as well as FAPEAL (Alagoas state research agency) for partial financial support.

[1] L. Gammaitoni, P. Hänggi, and P. Jung, Rev. Mod. Phys. **70**, 223 (1998).
[2] D. R. Chialvo, O. Calvo, D. L. Gonzalez, O. Piro, and G. V. Savino, Phys. Rev. E **65**, 050902 (2002).
[3] P. Balenzuela, H. Braun, and D. R. Chialvo, Contemp. Phys. **53**, 17 (2011).
[4] Y. V. Ushakov, A. A. Dubkov, and B. Spagnolo, Phys. Rev. E **81**, 041911 (2010).
[5] S. Martignoli and R. Stoop, Phys. Rev. Lett. **105**, 048101 (2010).
[6] Y. V. Ushakov, A. A. Dubkov, and B. Spagnolo, Phys. Rev. Lett. **107**, 108103 (2011).
[7] D. R. Chialvo, Chaos **13**, 1226 (2003).
[8] J. F. Schouten, R. J. Ritsma, and B. Lopes Cardozo, J. Acoust. Soc. Am. **34**, 1418 (1962).
[9] J. M. Buldu, D. R. Chialvo, C. R. Mirasso, M. C. Torrent, and J. Garcia-Ojalvo, Europhys. Lett. **64**, 178 (2003).
[10] O. Calvo and D. R. Chialvo, Int. J. Bifurcation Chaos **16**, 731 (2006).

[11] G. Van der Sande, G. Verschaffelt, J. Danckaert, and C. R. Mirasso, Phys. Rev. E **72**, 016113 (2005).
[12] A. Lopera, J. M. Buldú, M. C. Torrent, D. R. Chialvo, and J. García-Ojalvo, Phys. Rev. E **73**, 021101 (2006).
[13] M. Yousefi, Y. Barbarin, S. Beri, E. A. J. M. Bente, M. K. Smit, R. Notzel, and D. Lenstra, Phys. Rev. Lett. **98**, 044101 (2007).
[14] A. Pumir, V. Nikolski, M. Hörning, A. Isomura, K. Agladze, K. Yoshikawa, R. Gilmour, E. Bodenschatz, and V. Krinsky, Phys. Rev. Lett. **99**, 208101 (2007).
[15] Z. Le, V. Castro, W. B. Pardo, J. A. Walkenstein, M. Monti, and E. Rosa, Phys. Rev. E **75**, 056216 (2007).
[16] A. Pikovsky, M. Rosenblum, and J. Kurths, *Synchronization: A Universal Concept in Nonlinear Science* (Cambridge University Press, Cambridge, 2003).
[17] C. C. Olson, J. M. Nichols, J. V. Michalowicz, and F. Bucholtz, Chaos **21**, 023136 (2011).
[18] L. O. Chua, C. W. Wu, A. Huang, and G. Zhong, IEEE Trans. Circuits Systems **40**, 732 (1993).
[19] M. P. Kennedy, IEEE Trans. Circuits Systems **40**, 640 (1993).
[20] A. S. Anishchenko, M. A. Safonova, and L. O. Chua, Int. J. Bifurcation Chaos **4**, 441 (1994).
[21] O. Calvo, I. Gomes, C. R. Mirasso, and R. Toral, AIP Conf. Proc. **622**, 427 (2002).
[22] I. Gomes, C. R. Mirasso, R. Toral, and O. Calvo, Physica A **327**, 115 (2003).
[23] W. Korneta, I. Gomes, C. R. Mirasso, R. Toral, and O. Calvo, Physica D **219**, 93 (2006).